Modeling Compliant Grasps Exploiting Environmental Constraints

Gionata Salvietti[1], Monica Malvezzi[2], Guido Gioioso[1,2] and Domenico Prattichizzo[1,2].

***Abstract*— In this paper we present a mathematical framework to describe the interaction between compliant hands and environmental constraints during grasping tasks. In the proposed model, we considered compliance at wrist, joint and contact level. We modeled the general case in which the hand is in contact with the object and the surrounding environment. All the other contact cases can be derived from the proposed system of equations. We performed several numerical simulation using the SynGrasp Matlab Toolbox to prove the consistency of the proposed model. We tested different combinations of compliance as well as different reference inputs for the hand/arm system considered. This work has to be intended as a tool for compliant hand designer since it allows to tune compliance at different levels before the real hand realization. Furthermore, the same framework can be used for compliant hand simulation in order to study the interaction with the environmental constrains and to plan complex manipulation tasks.**

I. Introduction

Observing a person picking up a flat object off a table, it is easy to understand how our "grasp planner" is not very precise. A strategy often employed by humans is to place the fingertips on the table near to the object, and start to slide them interacting with the table surface (Fig. 1). In this way it becomes unnecessary to precisely regulate the distance of the hand from the surface. Instead, since the object rests on the table, the interaction with the table surface is exploited to place the fingers in an optimal grasping position. This approach is in contrast with most of the robotic grasp planners that try to determine possible contact points/regions and precise wrist position, provided that an accurate description of the object is available. In [1] the authors investigated the human grasp performance considering the interactions between the hand and the environment. They also presented several grasp strategies on two different robotic platforms. Each of the strategies was tailored to exploit constraints commonly present in real-world grasping problems. Similarly in [2], Kazemi et al. reported the results of human subjects grasping studies which show the extent and characteristics of the contact with the environment under different task conditions. A closed-loop hybrid grasping controller that mimics this interactive, contact-rich strategy was also tested using a a compliant 7-DoFs Barrett Whole-Arm Manipulator (WAM).

These preliminary results on replicating the human strategies to exploit the environmental constraints are one of the motivations that are steering the design of robotic hands from fully actuated stiff hands to more underactuated and compliant solutions [3]. Recently, several hands with compliance and underactuation have been proposed in the literature, for instance the Pisa/IIT hand [4], the SDM Hand [5] and the RBO Hand [6]. The Pisa/IIT Hand embodied the concept of adaptive synergies [7] using only one motor to jointly activate the 19 joints. Innovative articulations and ligaments replace conventional joint design. The SDM Hand presented by Dollar er al. uses polymeric materials to simultaneously create the rigid links and compliant joints of the gripper. Joints are coupled using tendons making the hand passively adaptable to the object physical properties. Finally, the RBO Hand uses a novel pneumatic actuator design in its fingers. These actuators are built entirely out of flexible materials and are thus inherently compliant. The air actuation system also make the hand highly adaptable to the grasped object.

Fig. 1. The human hand sliding on the table to grasp the charger.

This new family of underactuated and passively compliant hands guarantee robust grasping performance under sensing and actuation uncertainty. At this early stage, however, it is not clear how to design the hand/wrist stiffness to enhance the robot grasping and manipulation capability. We believe that to gain dexterity in advanced manipulation tasks using such compliant hands, it is necessary to understand how to fully exploit hand/object/environment interaction in order to plan the hand/arm motion. In other words, there is a need to model compliance at wrist, joint and contact level in order to design the new generation of underactuated hand and to plan complex manipulation tasks. Furthermore, there is a needing of modeling the environmental constraints to let the hands exploit them.

In this paper we introduce a mathematical framework to model compliant hands and their interaction with the environment. In particular, we extended the grasp analysis model presented in [8] to include compliance at wrist,

[1]Department of Advanced Robotics, Istituto Italiano di Tecnologia, Via Morego 30, 16163 Genoa, Italy. gionata.salvietti@iit.it

[2]Università degli Studi di Siena, Dipartimento di Ingegneria dell'Informazione, Via Roma 56, 53100 Siena, Italy. {malvezzi,gioioso,prattichizzo}@dii.unisi.it

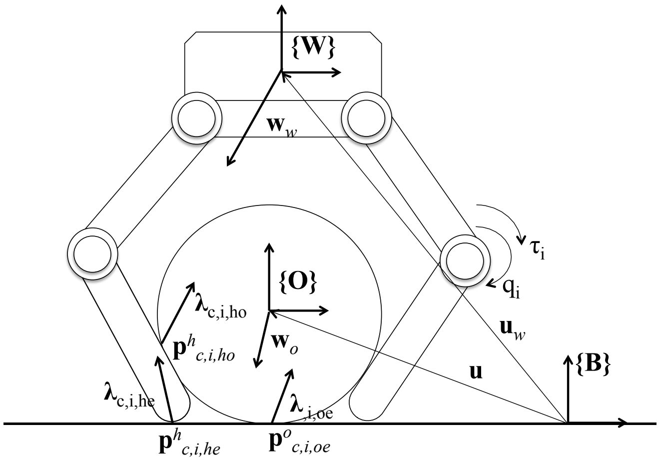

Fig. 2. A robotic hand interacting with an object and with the environment, main definitions.

joint and contact levels and to introduce the interaction with the environment. The model presented in this work describes the contact between hand and object, hand and environment and the different interactions between hand, object and environment. We propose numerical simulations to prove the consistency of the model. We analysed different combinations of compliance at wrist, joint and contact level varying the reference input for joint and wrist positions.

The final aim of this work is to give a simulation tool to test the compliance at different level in the new generation of underactuated hand, as well as to plan hand/arm compliant system trajectories that take advantages from the environmental constraints.

The rest of the paper is organized as it follows. In Section II the main equations regulating the model are introduced and described in details. Section III deals with the linearized solution to the equation system introduced in Section II. In Section IV the numerical simulation and the relative results are reported and discussed. Finally, in Section V conclusion and future work are outlined.

II. Modeling hand/object/environment interaction

In this section, we summarize the main assumption we made to obtain a mathematical model describing a compliant hand interacting with a surface and with an object. The main parameters that we adopted to define the system are summarized in Fig. 2.

One of the most important parts of the model is the description of the contact between the surfaces. In this preliminary work, we only consider a single point with friction contact model. The contacts between bodies are represented as points in which pure forces (without torques) are applied. With this simplification we can consider only the translation part of the relative motion between bodies at the contact points, without taking into account the rotation and than simplifying the notation. This procedure can be generalized

TABLE I
Possible Object/Environment/Hand configurations.

n.	**HE**	**OE**	**HO**	Scheme	Notes
1	NO	NO	YES	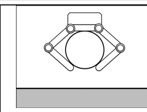	Hand Grasping
2	NO	YES	NO	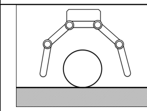	Approaching phase
3	NO	YES	YES	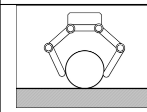	Obj./Env. interaction
4	YES	NO	YES	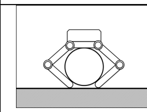	Hand/Env.+Hand/Obj
5	YES	YES	NO	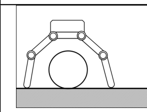	Hand/Env. interaction
6	YES	YES	YES	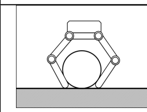	Most general case

for more complex contact models, for example including the spin moment, whose direction is around the normal direction to the contact surfaces at the contact point and whose magnitude depends on the relative rotation between contact bodies in this direction (this contact model is also referred as Soft Finger contact [9]).

Furthermore, to solve the force distribution problem, we introduce a compliant contact model: the contact surfaces are represented as locally deformable and we assume that the contact force is proportional to the local deformation [10], the proportionality constant is described by the contact stiffness matrix $\mathbf{K}_{c,i} \in \Re^{3\times3}$, that is assumed constant. More complex and reliable contact models are available in the literature [11], and will be considered in future improvements of this study.

We modeled robotic hand grasping exploiting the environmental constraints to reach and grasp the object. The environment is described as a surface Ψ whose shape is known in the base reference frame. Let $\Psi(\mathbf{p}) = 0$, $\Psi : \Re^3 \rightarrow \Re$ be its mathematical representation. Let $\{\mathbf{B}\}$ be a reference frame fixed with respect to the environment.

In the more general frame involving grasping with flexible hands exploiting environment constraints, three types of interaction (contact) can be identified:

- **HE**: hand/environment;
- **OE**: object/enviroment;
- **HO**: hand/object.

These three conditions can be combined to obtain up to eight possible configurations, the six more significant are summarized in Table I.

Let us consider the interaction between the hand and the environment. We suppose that each contact can be repre-

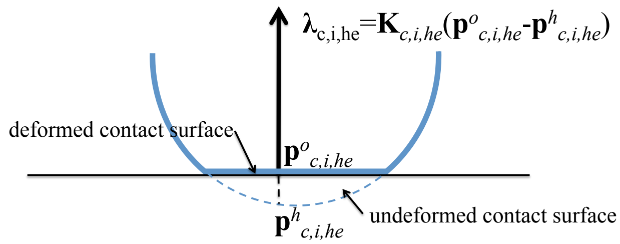

Fig. 3. Deformable contact surface: local deformation and contact force. The black line represents the environment surface, the blue one the hand finger surface.

sented as a point, let us indicate with $n_{he} \geq 0$ the number of contact points between the hand and the environment. According to the deformable contact model considered, we distinguish between the contact points on the hand and on the environment: let $\mathbf{p}_{c,i,he}^h, \mathbf{p}_{c,i,he}^e \in \Re^3$ be the coordinates of the i-th contact point on the hand and on the environment surfaces, respectively, expressed in $\{\mathbf{B}\}$ reference frame. In general, due to the local surface deformation, $\mathbf{p}_{c,i,he}^h \neq \mathbf{p}_{c,i,he}^e$, and the relative displacement between these two points is proportional to the contact force (see Fig. 3), i.e. $\boldsymbol{\lambda}_{c,i,he} = \mathbf{K}_{c,i,he}\left(\mathbf{p}_{c,i,he}^e - \mathbf{p}_{c,i,he}^h\right)$, where $\boldsymbol{\lambda}_{c,i,he} \in \Re^3$ is the contact force applied by the environment on the hand at the contact i, and $\mathbf{K}_{c,i,he} \in \Re^{3\times 3}$ is the contact stiffness matrix. We furthermore collect all the contact point coordinates and the contact forces in three vectors $\mathbf{p}_{c,he}^h, \mathbf{p}_{c,he}^e, \boldsymbol{\lambda}_{c,he} \in \Re^{3n_{he}}$, where $\mathbf{p}_{c,he}^h = \left[\mathbf{p}_{c,1,he}^{h\ \mathrm{T}}, \cdots, \mathbf{p}_{c,n_{he},he}^{h\ \mathrm{T}}\right]^{\mathrm{T}}$ and so on.

In the most general case, also the object interacts with the environment. Let us indicate with $n_{oe} \geq 0$ the number of contact points between the object and the environment. Also in this case, due to the local deformation of the hand and object surfaces due to the contact, we distinguish between the contact points on the object and on the environment theoretically undeformed surfaces: let $\mathbf{p}_{c,i,oe}^o, \mathbf{p}_{c,i,oe}^e \in \Re^3$ be the coordinates of the i-th contact point on the object and and on the environment, respectively, expressed in $\{\mathbf{B}\}$ reference frame. The object-environment contact force is given by $\boldsymbol{\lambda}_{c,i,oe} = \mathbf{K}_{c,i,oe}\left(\mathbf{p}_{c,i,oe}^e - \mathbf{p}_{c,i,oe}^o\right)$, where $\boldsymbol{\lambda}_{c,i,oe} \in \Re^3$ is the contact force applied by the environment on the object at the contact i, and $\mathbf{K}_{c,i,oe} \in \Re^{3\times 3}$ is the object/environment contact stiffness matrix. Also in this case we collect all the contact point coordinates and the contact forces in three vectors $\mathbf{p}_{c,oe}^o, \mathbf{p}_{c,oe}^e, \boldsymbol{\lambda}_{c,oe} \in \Re^{3n_{oe}}$.

Let us finally consider the interaction between the hand and the object. Let us indicate with $n_{ho} \geq 0$ the number of contact points between the hand and the object. Due to the local deformation of the contact surfaces, also in this case we distinguish between the contact points on the hand and on the object: let $\mathbf{p}_{c,i,ho}^h, \mathbf{p}_{c,i,ho}^o \in \Re^3$ be the coordinates of the i-th contact point on the hand and on the environment theoretical undeformed surfaces, respectively, expressed in $\{\mathbf{B}\}$ reference frame. The contact force is given by $\boldsymbol{\lambda}_{c,i,ho} = \mathbf{K}_{c,i,ho}\left(\mathbf{p}_{c,i,ho}^h - \mathbf{p}_{c,i,ho}^o\right)$, where $\boldsymbol{\lambda}_{c,i,ho} \in \Re^3$ is the contact force applied by the hand on the object at the contact i, and $\mathbf{K}_{c,i,ho} \in \Re^{3\times 3}$ is the contact stiffness matrix. We collect all the contact point coordinates and the contact forces in three vectors $\mathbf{p}_{c,ho}^h.\mathbf{p}_{c,ho}^o, \boldsymbol{\lambda}_{c,ho} \in \Re^{3n_{ho}}$, where $\mathbf{p}_{c,ho}^h = \left[\mathbf{p}_{c,1,ho}^{h\ \mathrm{T}}, \cdots, \mathbf{p}_{c,n_{ho},ho}^{h\ \mathrm{T}}\right]^{\mathrm{T}}$ and so on.

According to the previous definition, we can express the contact forces in the three contact types, as

$$\boldsymbol{\lambda}_{c,he} = \mathbf{K}_{c,he}\left(\mathbf{p}_{c,he}^e - \mathbf{p}_{c,he}^h\right) \tag{1}$$
$$\boldsymbol{\lambda}_{c,oe} = \mathbf{K}_{c,oe}\left(\mathbf{p}_{c,oe}^e - \mathbf{p}_{c,oe}^o\right) \tag{2}$$
$$\boldsymbol{\lambda}_{c,ho} = \mathbf{K}_{c,ho}\left(\mathbf{p}_{c,ho}^h - \mathbf{p}_{c,ho}^o\right), \tag{3}$$

where $\mathbf{K}_{c,he} \in \Re^{3n_{he}\times 3n_{he}}$, $\mathbf{K}_{c,oe} \in \Re^{3n_{oe}\times 3n_{oe}}$, $\mathbf{K}_{c,ho} \in \Re^{3n_{ho}\times 3n_{ho}}$ are the stiffness matrices including all the contact points. In the following we will analyse a *small* perturbation of system configuration from an initial equilibrium condition, and we will indicate with $\Delta\cdot$ the corresponding variation of a generic system variable "$\cdot$". If a *small* variation w.r.t. an initial equilibrium configuration is considered, equations (1-3) can be rewritten as

$$\Delta\boldsymbol{\lambda}_{c,he} = -\mathbf{K}_{c,he}\Delta\mathbf{p}_{c,he}^h \tag{4}$$
$$\Delta\boldsymbol{\lambda}_{c,oe} = -\mathbf{K}_{c,oe}\Delta\mathbf{p}_{c,oe}^o \tag{5}$$
$$\Delta\boldsymbol{\lambda}_{c,ho} = \mathbf{K}_{c,ho}\left(\Delta\mathbf{p}_{c,ho}^h - \Delta\mathbf{p}_{c,ho}^o\right). \tag{6}$$

The hand consists of a series of n_f serial kinematic chains, the fingers. Each finger has $n_{q,i}$, with $i = 1, \cdots, n_f$, degrees of freedom. We suppose that each finger can be represented as a series of $n_{q,i}$ links connected by $n_{q,i}$ one-degree-of freedom joints (revolute, R, or prismatic, P, joints). Let $n_q = \sum_{i=1}^{n_f} n_{q,i}$ be the total number of the hand degrees of freedom and let $\mathbf{q} \in \Re^{n_q}$ be the whole hand joint configuration vector, containing the values of all the hand joint displacements (a rotation for a revolute joint, a translation for the prismatic one). Typically in grasp theory and modeling literature, the fingers are connected to a common base (the hand palm) on which a fixed coordinate reference frame is defined. In this work, we suppose that the hand is connected to an arm through its palm that is not fixed. Furthermore we suppose that the whole arm/wrist system has a certain flexibility that is represented w.r.t. the wrist by the stiffness matrix $\mathbf{K}_w \in \Re^{6\times 6}$. Let us indicate with $\mathbf{u}_w \in \Re^6$ the generic six-dimensional displacement of the palm reference frame $\{\mathbf{W}\}$ with respect to the fixed base frame $\{\mathbf{B}\}$. The configuration vector $\mathbf{u}_w$ is a function of the arm kinematic structure and of the whole system flexibility. The whole hand configuration vector will be therefore described by the joint configuration $\mathbf{q}$ and the palm configuration $\mathbf{u}_w$. We can collect all these values in a unique vector $\tilde{\mathbf{q}} = \left[\mathbf{q}^{\mathrm{T}}, \mathbf{u}_w^{\mathrm{T}}\right]^{\mathrm{T}} \in \Re^{n_q+6}$. Let us indicate with $\boldsymbol{\tau} \in \Re^{n_q}$ the set of generalized forces (a force for each prismatic joint, a torque for each revolute joint) acting on hand joints, and with $\mathbf{w}_w$ the total wrench that the arm applies to the hand, expressed w.r.t. $\{\mathbf{B}\}$ frame origin point. We can thus collect all the actions on the hand in the vector $\tilde{\boldsymbol{\tau}} = \left[\boldsymbol{\tau}^{\mathrm{T}}, \mathbf{w}_w^{\mathrm{T}}\right]^{\mathrm{T}} \in \Re^{n_q+6}$.

From the kinematic analysis of the hand/arm system, we can express the position of the contact points as a function of hand/arm configuration. Considering the hand/environment interaction we get

$$\mathbf{p}^h_{c,he} = \boldsymbol{\kappa}_{he}(\tilde{\mathbf{q}}), \tag{7}$$

while, considering the hand/object interaction

$$\mathbf{p}^h_{c,ho} = \boldsymbol{\kappa}_{ho}(\tilde{\mathbf{q}}), \tag{8}$$

where $\boldsymbol{\kappa}_{he} : \Re^{n_q+6} \rightarrow \Re^{3n_{he}}$, $\boldsymbol{\kappa}_{ho} : \Re^{n_q+6} \rightarrow \Re^{3n_{ho}}$ are the direct kinematic relationships. The displacements of the contact points due to a small variation of the hand configuration is given by

$$\Delta\mathbf{p}^h_{c,he} = \tilde{\mathbf{J}}_{he}\Delta\tilde{\mathbf{q}}, \tag{9}$$

$$\Delta\mathbf{p}^h_{c,ho} = \tilde{\mathbf{J}}_{ho}\Delta\tilde{\mathbf{q}}, \tag{10}$$

where $\tilde{\mathbf{J}}_{he} \in \Re^{3n_{he}\times n_q+6}$ and $\tilde{\mathbf{J}}_{ho} \in \Re^{3n_{ho}\times n_q+6}$ are the complete Jacobian matrices, mapping hand configuration vector on contact point displacements. Complete hand Jacobian matrices can be evaluated as

$$\tilde{\mathbf{J}}_{he} = [\mathbf{J}_{h,he}, \mathbf{J}_{w,he}],$$

$$\tilde{\mathbf{J}}_{ho} = [\mathbf{J}_{h,ho}, \mathbf{J}_{w,ho}],$$

where $\mathbf{J}_{h,he}$, $\mathbf{J}_{h,ho}$ are the hand Jacobian matrices, that can be evaluated with the classical methods proposed for grasp analysis [8], [12], while $\mathbf{J}_{w,he}$, $\mathbf{J}_{w,ho}$ relating contact point displacement to hand palm displacement, are two matrices composed of n_{he} and n_{ho} (3×6) blocks $\mathbf{J}_{w,i}$ given by $\mathbf{J}_{w,i} = [\mathbf{I}_{3\times3}, -\mathbf{S}(\mathbf{p}_i - \mathbf{u}_w),]$. [1]

Applying the Principle of Virtual Work to the system composed of the hand connected to the arm and the environment, we get

$$\tilde{\boldsymbol{\tau}} = -\tilde{\mathbf{J}}^{\mathrm{T}}_{he}\boldsymbol{\lambda}_{c,he} + \tilde{\mathbf{J}}^{\mathrm{T}}_{ho}\boldsymbol{\lambda}_{c,ho}, \tag{11}$$

mapping the contact forces to the joint torques and palm wrench. If we consider a small perturbation from an initial equilibrium condition, we can linearize the above static relationship, obtaining

$$\Delta\tilde{\boldsymbol{\tau}} = -\tilde{\mathbf{J}}^{\mathrm{T}}_{he}\Delta\boldsymbol{\lambda}_{c,he} + \tilde{\mathbf{J}}^{\mathrm{T}}_{ho}\Delta\boldsymbol{\lambda}_{c,ho} + \mathbf{H}\Delta\tilde{\mathbf{q}}, \tag{12}$$

where

$$\mathbf{H} = \frac{\partial\tilde{\mathbf{J}}^{\mathrm{T}}_{he}\boldsymbol{\lambda}_{he}}{\partial\tilde{\mathbf{q}}} + \frac{\partial\tilde{\mathbf{J}}^{\mathrm{T}}_{ho}\boldsymbol{\lambda}_{ho}}{\partial\tilde{\mathbf{q}}}.$$

$\mathbf{H} \in \Re^{(n_q+6)\times(n_q+6)}$ takes into account the variation of Jacobian matrices with respect to hand configuration. This term is present when in the initial equilibrium condition the system is *loaded*, i.e. $\boldsymbol{\lambda}_{c,he} \neq 0$ and/or $\boldsymbol{\lambda}_{c,ho} \neq 0$. In this paper we suppose that the hand and the arm are controlled in position with a proportional controller. The hand and arm system are not perfectly stiff and can be described by means of a compliant model. The flexibility is in the more general case due to: (1) the gain of the proportional position control of hand joints and wrist position, (2) the flexibility of the joints, and (3) the flexibility of the links, that can be represented in the joint space [13]. The torque applied to hand joints and the wrench applied to the wrist are proportional to the difference between the reference and actual hand/arm configuration, i.e.

$$\tilde{\boldsymbol{\tau}} = \tilde{\mathbf{K}}_q\left(\tilde{\mathbf{q}}_r - \tilde{\mathbf{q}}\right) + \tilde{\boldsymbol{\tau}}_0, \tag{13}$$

where $\tilde{\mathbf{q}}_r = \left[\mathbf{q}^{\mathrm{T}}_r, \mathbf{u}^{\mathrm{T}}_{r,w}\right]^{\mathrm{T}} \in \Re^{n_q+6}$ is a vector containing the reference hand joint displacements $\mathbf{q}_r$ and the reference palm configuration $\mathbf{u}_{r,w}$, and

$$\tilde{\mathbf{K}}_q = \begin{bmatrix} \mathbf{K}_q & \mathbf{0} \\ \mathbf{0} & \mathbf{K}_w \end{bmatrix}.$$

$\mathbf{K}_q \in \Re^{n_q\times n_q}$ is the joint stiffness matrix, while $\mathbf{K}_w \in \Re^{6\times6}$, previously introduced, represents the stiffness of the connection between the hand and the arm and thus takes into account the stiffness of the whole arm. Both the matrices are symmetric and positive. If we consider a small variation with respect to a reference equilibrium configuration we get

$$\Delta\tilde{\boldsymbol{\tau}} = \tilde{\mathbf{K}}_q\left(\Delta\tilde{\mathbf{q}}_r - \Delta\tilde{\mathbf{q}}\right). \tag{14}$$

Let us consider the interaction between the environment and the object. The position of the i-th contact point on the object can be expressed as

$$\mathbf{p}^o_{c,i,eo} = \mathbf{p}_o + \mathbf{R}^B_o\mathbf{p}^o_{c,i,eo}, \tag{15}$$

where $\mathbf{p}_o$ represents the coordinates of $\{\mathbf{O}\}$ reference frame origin w.r.t. $\{\mathbf{B}\}$, $\mathbf{R}^B_o$ is the rotation matrix between $\{\mathbf{O}\}$ and $\{\mathbf{B}\}$, $\mathbf{p}^o_{c,i,eo}$ are the coordinates of the i-th contact points in the $\{\mathbf{O}\}$ frame. If we consider a small displacement, the following relationship can be written

$$\Delta\mathbf{p}^o_{c,i,eo} = \Delta\mathbf{p}_o - \mathbf{S}(\mathbf{p}^o_{c,i,eo} - \mathbf{p}_o)\Delta\boldsymbol{\phi}, \tag{16}$$

where $\Delta\boldsymbol{\phi} = [\Delta\phi_x, \Delta\phi_y, \Delta\phi_z]^{\mathrm{T}}$ represents the relative elementary rotation between $\{\mathbf{O}\}$ and $\{\mathbf{B}\}$. This equation can be synthesized as

$$\Delta\mathbf{p}^o_{c,i,eo} = \mathbf{G}^{\mathrm{T}}_{i,eo}\Delta\mathbf{u}, \tag{17}$$

with $\mathbf{u} = \left[\Delta\mathbf{p}^{\mathrm{T}}_o, \Delta\boldsymbol{\phi}^{\mathrm{T}}\right]^{\mathrm{T}}$, and

$$\mathbf{G}^{\mathrm{T}}_{eo} = \left[\mathbf{I}, -\mathbf{S}(\mathbf{p}^o_{c,i,eo} - \mathbf{p}_o)\right].$$

Extending this kinematic relationship to all the contact points we get

$$\Delta\mathbf{p}^o_{c,eo} = \mathbf{G}^{\mathrm{T}}_{eo}\Delta\mathbf{u}, \tag{18}$$

where

$$\mathbf{G}^{\mathrm{T}}_{eo} = \begin{bmatrix} \mathbf{G}^{\mathrm{T}}_{1,eo} \\ \cdots \\ \mathbf{G}^{\mathrm{T}}_{n_{eo},eo} \end{bmatrix}.$$

Similarly, considering the contacts between the hand and the object, the following relationship can be written

$$\Delta\mathbf{p}^o_{c,ho} = \mathbf{G}^{\mathrm{T}}_{ho}\Delta\mathbf{u}, \tag{19}$$

where $\mathbf{G}^{\mathrm{T}}_{ho} \in \Re^{3n_{ho}\times6}$ is the Grasp Matrix [9]. By applying the Principle of Virtual Works to the object, the following relationship describing object static equilibrium can be obtained

$$\mathbf{w}_o = -\mathbf{G}_{eo}\boldsymbol{\lambda}_{c,eo} + \mathbf{G}_{ho}\boldsymbol{\lambda}_{c,ho}, \tag{20}$$

[1] $\mathbf{S}(\mathbf{v})$ represents the skew matrix corresponding to the vector $\mathbf{v}$.

where $\mathbf{w}_o \in \Re^6$ is the external wrench applied to the object. If a small perturbation w.r.t. an initial equilibrium configuration is considered, the static equilibrium in the new configuration is described by

$$\Delta\mathbf{w}_o = -\mathbf{G}_{eo}\Delta\boldsymbol{\lambda}_{c,eo} + \mathbf{G}_{ho}\Delta\boldsymbol{\lambda}_{c,ho} + \mathbf{L}\Delta\mathbf{u}, \tag{21}$$

where

$$\mathbf{L} = -\frac{\partial \mathbf{G}_{eo}\boldsymbol{\lambda}_{c,eo}}{\partial \mathbf{u}} + \frac{\partial \mathbf{G}_{ho}\boldsymbol{\lambda}_{c,ho}}{\partial \mathbf{u}}.$$

$\mathbf{L} \in \Re^{6\times 6}$ takes into account the variation of $\mathbf{G}_{eo}$ and $\mathbf{G}_{ho}$ with respect to object displacement. It can be neglected if in the initial reference configuration the system is unloaded, i.e. if $\boldsymbol{\lambda}_{c,eo} = \mathbf{0}$ and $\boldsymbol{\lambda}_{c,ho} = \mathbf{0}$, or if the matrices do not depend on $\mathbf{u}$. This condition can be obtained by expressing contact displacements and contact forces w.r.t. $\{\mathbf{O}\}$ reference frame and assuming that the contact points are fixed on the object.

Summarizing all the equations describing a small variation of system configuration w.r.t. an initial equilibrium configuration, the following homogeneous linear system can be obtained

$$\left\{\begin{array}{lcl}
\Delta\boldsymbol{\lambda}_{c,he} + \mathbf{K}_{c,he}\Delta\mathbf{p}^h_{c,he} & = & 0\\
\Delta\boldsymbol{\lambda}_{c,oe} + \mathbf{K}_{c,oe}\Delta\mathbf{p}^o_{c,oe} & = & 0\\
\Delta\boldsymbol{\lambda}_{c,ho} - \mathbf{K}_{c,ho}\Delta\mathbf{p}^h_{c,ho} + \mathbf{K}_{c,ho}\Delta\mathbf{p}^o_{c,ho} & = & 0\\
\Delta\mathbf{p}^h_{c,he} - \tilde{\mathbf{J}}_{he}\Delta\tilde{\mathbf{q}} & = & 0\\
\Delta\mathbf{p}^h_{c,ho} - \tilde{\mathbf{J}}_{ho}\Delta\tilde{\mathbf{q}} & = & 0\\
\Delta\tilde{\boldsymbol{\tau}} + \tilde{\mathbf{J}}^{\mathrm{T}}_{he}\Delta\boldsymbol{\lambda}_{c,he} - \tilde{\mathbf{J}}^{\mathrm{T}}_{ho}\Delta\boldsymbol{\lambda}_{c,ho} - \mathbf{H}\Delta\tilde{\mathbf{q}} & = & 0\\
\Delta\tilde{\boldsymbol{\tau}} - \tilde{\mathbf{K}}_q\Delta\tilde{\mathbf{q}}_r + \tilde{\mathbf{K}}_q\Delta\tilde{\mathbf{q}} & = & 0\\
\Delta\mathbf{p}^o_{c,ho} - \mathbf{G}^{\mathrm{T}}_{ho}\Delta\mathbf{u} & = & 0\\
\Delta\mathbf{p}^o_{c,eo} - \mathbf{G}^{\mathrm{T}}_{eo}\Delta\mathbf{u} & = & 0\\
\Delta\mathbf{w}_o + \mathbf{G}_{eo}\Delta\boldsymbol{\lambda}_{c,eo} - \mathbf{G}_{ho}\Delta\boldsymbol{\lambda}_{c,ho} - \mathbf{L}\Delta\mathbf{u} & = & 0
\end{array}\right. \tag{22}$$

III. LINEARIZED SOLUTION

The linear system in eq. (22) can be written in this form

$$\mathbf{A}\Delta\boldsymbol{\xi} = \Delta\boldsymbol{\upsilon}, \tag{23}$$

where

$$\Delta\boldsymbol{\xi} = \left[\Delta\boldsymbol{\lambda}^{\mathrm{T}}, \Delta\mathbf{p}_c^{\mathrm{T}}, \Delta\tilde{\mathbf{q}}^{\mathrm{T}}, \Delta\tilde{\boldsymbol{\tau}}^{\mathrm{T}}, \Delta\mathbf{u}^{\mathrm{T}}\right]^{\mathrm{T}},$$

with

$$\Delta\boldsymbol{\lambda}^{\mathrm{T}} = \left[\Delta\boldsymbol{\lambda}^{\mathrm{T}}_{c,he}, \Delta\boldsymbol{\lambda}^{\mathrm{T}}_{c,oe}, \Delta\boldsymbol{\lambda}^{\mathrm{T}}_{c,ho}\right],$$

$$\Delta\mathbf{p}_c^{\mathrm{T}} = \left[\Delta\mathbf{p}^{h\mathrm{T}}_{c,he}, \Delta\mathbf{p}^{o\mathrm{T}}_{c,oe}, \Delta\mathbf{p}^{h\mathrm{T}}_{c,ho}, \Delta\mathbf{p}^{o\mathrm{T}}_{c,ho}\right].$$

The matrix $\mathbf{A}$ is square so, if it is not singular, the linear system can be solved to find $\Delta\boldsymbol{\xi}$.

The solution of the linear system in eq. (22), obtained with $\Delta\mathbf{w}_o = 0$, $\Delta\tilde{\mathbf{q}} \neq 0$ allows to understand, for a given configuration, which are the possible controllable forces and movements that can be obtained acting on hand and arm reference configuration [10]. The solution can be expressed as

$$\begin{array}{rcl}
\Delta\boldsymbol{\lambda} & = & \mathbf{V}_q\Delta\tilde{\mathbf{q}}_r,\\
\Delta\mathbf{p}_c & = & \mathbf{P}_q\Delta\tilde{\mathbf{q}}_r,\\
\Delta\tilde{\mathbf{q}} & = & \mathbf{Q}_q\Delta\tilde{\mathbf{q}}_r,\\
\Delta\tilde{\boldsymbol{\tau}} & = & \mathbf{T}_q\Delta\tilde{\mathbf{q}}_r,\\
\Delta\mathbf{u} & = & \mathbf{U}_q\Delta\tilde{\mathbf{q}}_r.
\end{array} \tag{24}$$

Each of the above matrices can be partitioned in order to highlight the contribution of arm reference variation and hand joint reference variation in the whole result. For instance, the actual joint configuration $\Delta\tilde{\mathbf{q}}$ can be expressed as follows

$$\left[\begin{array}{c}\Delta\mathbf{q}\\ \Delta\mathbf{u}_w\end{array}\right] = \left[\begin{array}{cc}\mathbf{Q}_{qq} & \mathbf{Q}_{qu}\\ \mathbf{Q}_{uq} & \mathbf{Q}_{uu}\end{array}\right]\left[\begin{array}{c}\Delta\mathbf{q}_r\\ \Delta\mathbf{u}_{w,r}\end{array}\right]$$

where $\mathbf{Q}_{qq}$ describes hand joint variation $\Delta\mathbf{q}$ when the reference values of hand joints are varied and the hand palm reference displacement is constant, $\mathbf{Q}_{qu}$ describes hand joint variation $\Delta\mathbf{q}$ when the reference values of hand palm reference displacement is varied, while the reference values of the hand joints are constant, and so on.

The solution of the linear system in eq. (22) when $\Delta\mathbf{w}_o \neq 0$ and $\Delta\tilde{\mathbf{q}} = 0$ allows to investigate on how the system is able to resist to external disturbances, represented as variations of the wrench applied to the object. The solution in this case can be expressed as

$$\begin{array}{rcl}
\Delta\boldsymbol{\lambda} & = & \mathbf{V}_w\Delta\mathbf{w}_o,\\
\Delta\mathbf{p}_c & = & \mathbf{P}_w\Delta\mathbf{w}_o,\\
\Delta\tilde{\mathbf{q}} & = & \mathbf{Q}_w\Delta\mathbf{w}_o,\\
\Delta\tilde{\boldsymbol{\tau}} & = & \mathbf{T}_w\Delta\mathbf{w}_o,\\
\Delta\mathbf{u} & = & \mathbf{U}_w\Delta\mathbf{w}_o.
\end{array} \tag{25}$$

In particular, $\mathbf{K}_{grasp} = \mathbf{U}_w^{-1}$ maps the variation of the external wrench applied to the object to object displacement. It is the generalization of the Grasp Stiffness matrix defined in [14], [15], [16] to hands grasping an object and interacting with a surface.

Solution for the sub-problems

The above presented solution is relative to the more general case, in which a contact exists between the hand and the object, the hand and the environment surface, and the object and the environment. This case is indicated with number 6 in Table I. A linear system can be similarly obtained in all the other cases, by choosing the proper equations and unknowns from the system in eq. (22). For instance, the equations that have to be solved in the case indicated with number 5 in Table I, i.e. hand/environment and object/environment interaction, are

$$\left\{\begin{array}{lcl}
\Delta\boldsymbol{\lambda}_{c,he} + \mathbf{K}_{c,he}\Delta\mathbf{p}^h_{c,he} & = & 0\\
\Delta\boldsymbol{\lambda}_{c,oe} + \mathbf{K}_{c,oe}\Delta\mathbf{p}^o_{c,oe} & = & 0\\
\Delta\mathbf{p}^h_{c,he} - \tilde{\mathbf{J}}_{he}\Delta\tilde{\mathbf{q}} & = & 0\\
\Delta\tilde{\boldsymbol{\tau}} + \tilde{\mathbf{J}}^{\mathrm{T}}_{he}\Delta\boldsymbol{\lambda}_{c,he} - \mathbf{H}\Delta\tilde{\mathbf{q}} & = & 0\\
\Delta\tilde{\boldsymbol{\tau}} - \tilde{\mathbf{K}}_q\Delta\tilde{\mathbf{q}}_r + \tilde{\mathbf{K}}_q\Delta\tilde{\mathbf{q}} & = & 0\\
\Delta\mathbf{p}^o_{c,eo} - \mathbf{G}^{\mathrm{T}}_{eo}\Delta\mathbf{u} & = & 0\\
\Delta\mathbf{w}_o + \mathbf{G}_{eo}\Delta\boldsymbol{\lambda}_{c,eo} - \mathbf{L}\Delta\mathbf{u} & = & 0
\end{array}\right. \tag{26}$$

All the cases in Table I can be thus derived with the same approach. The proposed procedure can be adopted to evaluate and analyse, for a given configuration, the main grasp properties. Even if eq. (22) and (26), represent a linear quasi–static approximation of the generally nonlinear equations describing the system dynamics, they can be the basis of a procedure for grasping simulation.

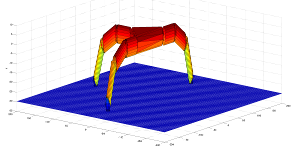

(a) Modular hand, initial configuration.

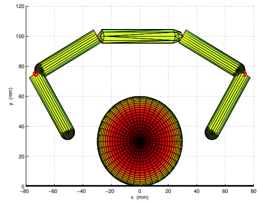

(b) Planar gripper, initial configuration.

Fig. 4. Starting configurations for the simulation of the modular 3-fingered hand and of the planar 4DoFs gripper.

IV. Numerical Simulation

The proposed linear quasi–static model has been implemented and verified by means of several numerical simulations using SynGrasp [17]. SynGrasp is a Matlab Toolbox for the simulation and the analysis of grasping in which several hand models are available. It also includes functions for the definition of hand kinematic structure and of the contact points with a grasped object, the coupling between joints induced by a synergistic control, compliance at the contact, joint and actuator levels. For this work, we integrated the hand models available considering also compliance at wrist level and the contact with a fixed surface. In particular, we used the models of a 4 DoFs planar gripper and a three-fingered modular hand. The gripper is composed of 2 symmetric 2 DoFs fingers, whose link lengths are 50 mm and whose base length is 60 mm. The links are connected each other and to the base by 4 revolute joints with parallel axes, so that the mechanism is planar. Concerning the modular hand, each module $(42 \times 33 \times 16)$mm has one DoF and it is connected to the others obtaining kinematic chains that we consider as fingers. These chains are connected to a common base defined as a palm. In the proposed configuration each finger has three DoFs, thus the hand has globally nine DoFs. The main goal of the numerical simulations was to verify the behavior of the compliant hands during the interaction with objects and environment. In particular, in the first set of simulations we considered the modular hand interaction only with the environment, while in the second set the gripper is interacting both with the object and the environmental constraints.

A. Modular hand interacting with the environment

In the first set of simulations we focused on the interaction between a compliant modular hand, and an environmental constraint represented by a flat surface, e.g., a table. We considered the modular hand already in contact with the table at the beginning of the simulations. The initial configuration of the hand joint vector is $\mathbf{q}_{init} = \left[\begin{array}{ccccccccc} 0 & 0.2 & 0.6 & 0 & 0.2 & 0.6 & 0 & 0.2 & 0.6 \end{array} \right]$ rad. The hand in the initial configuration is reported in Fig. 4. We tested different combination of compliance values and reference inputs. The result showed in Fig. 5 are obtained using a fixed reference input

$$\Delta\mathbf{q}_r = \left[\begin{array}{ccccccccc} 0.1 & 0 & 0 & 0.1 & 0 & 0 & 0.1 & 0 & 0 \end{array} \right],$$

for 20 simulation steps. This reference input results in the motion of the joints more close to the palm of all the fingers. The six components of the vector representing the wrist reference input, was set to zero in this case. We set the following contact stiffness values

$$\mathbf{K}_{c,he} = k_c \mathbf{I}_{3\times n_{he}},\ \mathbf{K}_w = k_w \mathbf{I}_{6\times 6},\ \mathbf{K}_q = k_q \mathbf{I}_{n_q \times n_q}.$$

In Fig. 5-a we used $k_c = 1000$ N/mm, $k_q = 1000$ Nmm/rad and $k_w = 0.001$ N/mm, simulating a stiff hand interacting with a stiff surface and connected to a flexible arm. Since the both hand joints and contact have an high stiffness the reference input produce a displacement of the wrist toward the direction perpendicular to the table. In Fig. 5-b we tested the behavior of the hand when the joint stiffness in much lower that the contact stiffness. We set $k_c = 1000$ N/mm, $k_q = 1$ Nmm/rad, and $k_w = 1$ N/mm. From the results we can observe a bigger deformation of the hand. Finally in Fig. 5-c we simulated a soft contact with a stiff hand. The coefficients where fixed to $k_c = 1$ N/mm, $k_q = 1000$ Nmm/rad and $k_w = 1$ N/mm. We did not represent the deformation of the table: in the diagram a penetration of the hand fingers onto the constraint surface can be observed.

In the second set of simulations, we tested different wrist compliance values choosing as reference joint vector components the following values

$$\Delta\mathbf{u}_{w,r} = \left[\begin{array}{cccccc} 0 & 0 & -0.2 & 0 & 0 & 0 \end{array} \right],$$

which corresponds to a motion of the hand toward the table without closing the hand joints, whose reference vector was set to zero. In Fig. 6-a we considered $k_w = 0.001$ N/mm, while in Fig. 6-b k_w was equal to 1 N/mm. The other coefficients where kept fixed at $k_c = 1000$ N/mm, $k_q = 10$ Nmm/rad. As expected in the case with high wrist stiffness, the hand deforms, since the palm is pushed toward the table and the hand joints are compliant. In the second case, when the wrist stiffness is low, all the motion is “captured” by the wrist producing an almost zero effect in the hand joints.

B. Planar gripper interacting with the environment and with an object.

The second numerical example is realized with the model of a planar 4 DoFs gripper, whose SynGrasp representation in the initial configuration is shown in Fig. 4(b). During the simulation, in the first phase the gripper moves towards the flat surface, by changing wrist reference configuration, Fig. 7(a). Once the contact with the surface is reached, the gripper is closed by acting on the reference values of the proximal joints (Fig. 7(b)), until the gripper links reaches the object (Fig. 7(c)). In the final part of the simulation, (Fig. 7(d)) the gripper interacts both with the surface and with the object: the reference values of the proximal joints are increased until the object is lifted up.

The gripper is planar and has two fingers, each finger is composed of two phalanges with the same lengths $a =$ 50 mm. Let $J_1, \cdots, J_4$ be the joint axis traces on the gripper plane, and let $\theta_1, \cdots, \theta_4$ be the joint angles. A fixed reference frame $\{\mathbf{B}\}$ is fixed on a flat horizontal surface that represents the environment. The y axis is supposed

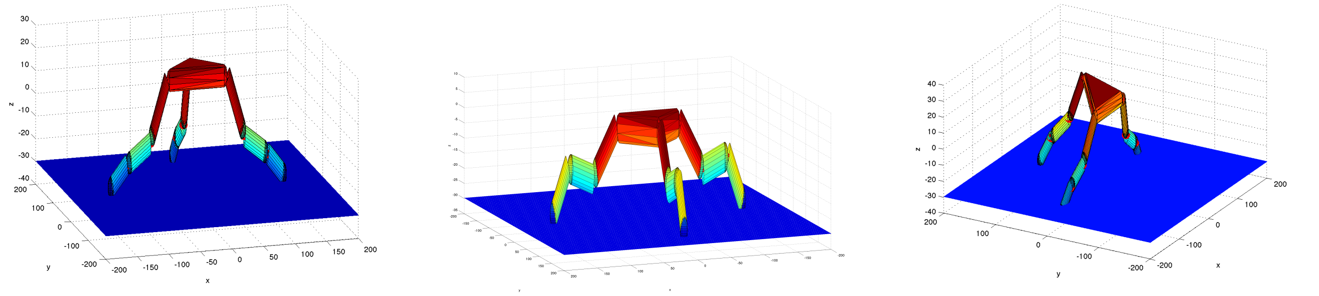

(a) The modular hand interacting with a plane with high joint stiffness and low contact stiffness. (b) The modular hand interacting with a plane with low joint stiffness and high contact stiffness. (c) The modular hand interacting with a plane with high joint stiffness and low contact stiffness.

Fig. 5. Different hand configuration obtained varying compliance at joint and contact level.

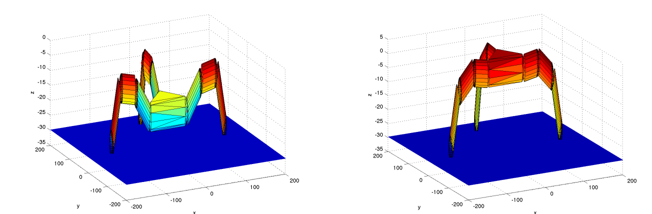

(a) The modular hand interacting with a plane with high wrist stiffness and low joint stiffness. (b) The modular hand interacting with a plane with low wrist stiffness and low joint stiffness.

Fig. 6. Different hand configuration obtained varying compliance at wrist level.

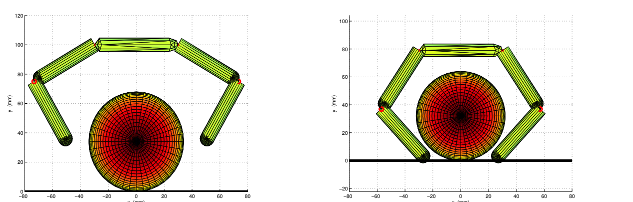

(a) Initial configuration. (b) The gripper reaches the environment surface.

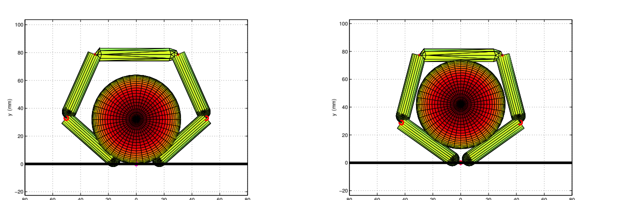

(c) The gripper slides on the surface until it reaches the object. (d) The gripper grasps the object.

Fig. 7. Four steps of the simulated grasping.

orthogonal to the surface. Let $\mathbf{W}$ a reference frame on the gripper base, let $\mathbf{u}_w = [u_{w,x}, u_{wy}]^{\mathrm{T}}$ be the coordinates of its origin w.r.t $\{\mathbf{B}\}$, and let ϕ the angle between x axes. In this simulation, we suppose that the gripper interacts with a the horizontal plane $y = 0$ and with a spherical object, with radius $r = 30$ mm, whose center O has coordinates $\mathbf{u}_o = [0, r]$ w.r.t. $\{\mathbf{B}\}$.

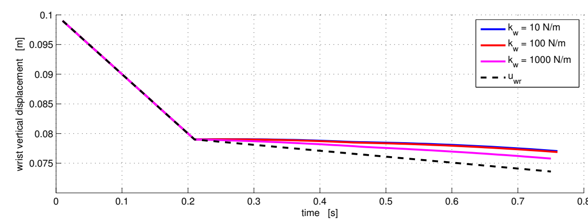

(a) Vertical displacement of the wrist, for different values of k_w.

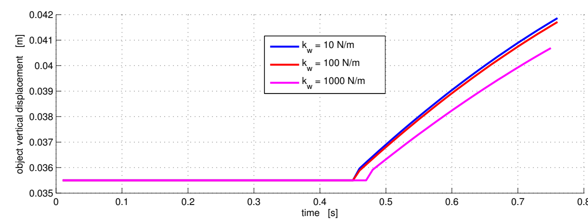

(b) Vertical displacement of the object, for different values of k_w.

Fig. 8. Vertical displacement of the wrist and of the object during the simulation, for different values of wrist stiffness k_w.

In the initial configuration, the gripper is over the surface and does not interact neither with the surface nor with the object. We considered the following initial reference configuration for the gripper joints: $\theta_1 = \frac{\pi}{6}$ rad, $\theta_2 = \frac{\pi}{2}$ rad, $\theta_3 = \frac{\pi}{6}$ rad, $\theta_4 = \frac{\pi}{2}$ rad, the load applied to the object is $w_0 = 0$ N. In the first simulation phase the gripper wrist is moved to reach the environment surface and at the same time the reference values of the gripper joints are increased so that the gripper closes. When the gripper reaches the plane the joint angles are $\theta_1 = 1$ rad, $\theta_2 = 1.3$ rad, $\theta_3 = 1$ rad, $\theta_4 = 1.3$ rad,

When the gripper reaches the surface, due to the system geometry, the contact points correspond to the fingertips, let us indicate them with T_1 and T_2 and let us indicate with $\mathbf{t}_1, \mathbf{t}_2 \in \Re^2$ their coordinates. The hand/environment Jacobian matrix can be evaluated in this case as

$$\mathbf{J}_e = \begin{bmatrix} J_{e,1,1} & J_{e,1,2} & 0 & 0 & 1 & 0 & -t_{1,y} + u_{w,y} \\ J_{e,2,1} & J_{e,2,2} & 0 & 0 & 0 & 1 & t_{1,x} - u_{w,x} \\ 0 & 0 & J_{e,3,3} & J_{e,3,4} & 1 & 0 & -t_{2,y} + u_{w,y} \\ 0 & 0 & J_{e,4,3} & J_{e,4,4} & 0 & 1 & t_{2,x} - u_{w,x} \end{bmatrix}$$

in which the matrix terms can be expressed as:

$$\begin{array}{rcl} J_{e,1,1} & = & s\phi(ac_{12}+ac_1)-c\phi(as_{12}+as_1) \\ J_{e,1,2} & = & ac_{12}s\phi - as_{12}c\phi \end{array}$$

etc., with $s_1 = \sin\theta_1$, $c_1 = \cos\theta_1$, $s_{12} = \sin(\theta_1+\theta_2)$, and so on.

Once the gripper reaches the contact surface, we started to close it by increasing the reference values of θ_1 and θ_2 angles, until the object is reached. The contact points are indicated with C_1 and C_2, let $\mathbf{c}_1, \mathbf{c}_2$ be their coordinates, and let l_1 and l_2 be the distances from J_2 and J_4, respectively. The object center coordinates and object orientation are defined with respect to the base reference system by the vector $u = [u_x \quad u_y \quad \phi]^{\mathrm{T}}$, where ϕ represents the angle between the local and base reference systems abscissae axes. The hand/environment Jacobian matrix can be evaluated in this case as

$$\mathbf{J}_o = \begin{bmatrix} J_{o,1,1} & J_{o,1,2} & 0 & 0 & 1 & 0 & -c_{1,y}+u_{w,y} \\ J_{o,2,1} & J_{o,2,2} & 0 & 0 & 0 & 1 & c_{1,x}-u_{w,x} \\ 0 & 0 & J_{o,3,3} & J_{o,3,4} & 1 & 0 & -c_{2,y}+u_{w,y} \\ 0 & 0 & J_{o,4,3} & J_{o,4,4} & 0 & 1 & c_{2,x}-u_{w,x} \end{bmatrix},$$

in which the matrix terms can be expressed as

$$\begin{array}{rcl} J_{o,1,1} & = & s\phi(l_1c_{12}+ac_1)-c\phi(l_1s_{12}+as_1) \\ J_{o,1,2} & = & l_1c_{12}s\phi - l_1s_{12}c\phi \end{array},$$

etc.. The hand/object grasp matrix is given by

$$\mathbf{G}_o = \begin{bmatrix} 1 & 0 & 1 & 0 \\ 0 & 1 & 0 & 1 \\ -c_{1,y}+u_y & c_{1,x}-u_x & -c_{2,y}+u_y & c_{2,x}-u_x \end{bmatrix}.$$

The geometric terms, are considered by defining the matrices $\mathbf{H}$ and $\mathbf{L}$, that can be evaluated as a function of $\mathbf{J}_e$, $\mathbf{J}_o$ and $\mathbf{G}_o$ derivatives. Their expressions are not reported here for the sake of brevity.

Different simulations were performed changing, also in this case, the values of system stiffness. Fig. 8 shows, for different values of wrist stiffness, the corresponding wrist and object vertical displacement. As expected, during the sliding phase, the wrist displacement decreases as wrist stiffness increases.

V. Conclusion

The diffusion of underactuated and compliant robotic hands and the need of operating in unstructured and uncertain environments is leading to grasp planning procedures in which the robustness and adaptability is more important than precision and accuracy. In this framework, an interesting grasping strategy could be based on the exploitation of environmental constraints, which could be seen as support for the robotic hand, rather than an obstacle to be avoided. In this paper we proposed a mathematical representation of robotic grasping in which a compliant hand exploits the environment surface to reach the object in a reliable and robust way. Using this model the user is able to evaluate the main grasp properties, taking into account the interaction between the hand and the object, the object and the environment, the hand and the environment. In particular, the effect of hand and arm properties can be evaluated: the proposed model can be used in the design phase to define hand properties necessary to obtain the desired performance during grasping operations involving the exploitation of environmental constraints. Future development of the study will be devoted to define a more general description including dynamics effects and rolling between contact surfaces, and a more detailed description of contact model, including friction limits. The SynGrasp functions developed for this work are available on-line at http://syngrasp.dii.unisi.it.

References

[1] R. Deimel, C. Eppner, J. Alvarez-Ruiz, M. Maertens, and O. Brock, "Exploitation of environmental constraints in human and robotic grasping," in *International Symposium on Robotic Research*, 2013.

[2] M. Kazemi, J.-S. Valois, J. A. Bagnell, and N. Pollard, "Human-inspired force compliant grasping primitives," *Autonomous Robots*, vol. 37, no. 2, pp. 209–225, 2014.

[3] A. Bicchi and D. Prattichizzo, "Analysis and optimization of tendinous actuation for biomorphically designed robotic systems," *Robotica*, vol. 18, no. 1, pp. 23–31, 2000.

[4] M. G. Catalano, G. Grioli, E. Farnioli, A. Serio, C. Piazza, and A. Bicchi, "Adaptive synergies for the design and control of the pisa/iit softhand," *The International Journal of Robotics Research*, vol. 33, no. 5, pp. 768–782, 2014.

[5] A. M. Dollar and R. D. Howe, "The highly adaptive sdm hand: Design and performance evaluation," *The international journal of robotics research*, vol. 29, no. 5, pp. 585–597, 2010.

[6] R. Deimel and O. Brock, "A compliant hand based on a novel pneumatic actuator," in *Robotics and Automation (ICRA), 2013 IEEE International Conference on*, pp. 2047–2053, IEEE, 2013.

[7] G. Grioli, M. Catalano, E. Silvestro, S. Tono, and A. Bicchi, "Adaptive synergies: an approach to the design of under-actuated robotic hands," in *Intelligent Robots and Systems (IROS), 2012 IEEE/RSJ International Conference on*, pp. 1251–1256, IEEE, 2012.

[8] D. Prattichizzo, M. Malvezzi, M. Gabiccini, and A. Bicchi, "On motion and force controllability of precision grasps with hands actuated by soft synergies," *IEEE Transactions on Robotics*, vol. in press, pp. 1–17, 2013.

[9] D. Prattichizzo and J. Trinkle, "Grasping," in *Handbook on Robotics* (B. Siciliano and O. Kathib, eds.), pp. 671–700, Springer, 2008.

[10] A. Bicchi, "Force distribution in multiple whole-limb manipulation," in *Proc. IEEE Int. Conf. Robotics and Automation*, (Atlanta), pp. 196–201, 1993.

[11] K. L. Johnson, *Contact mechanics*. Cambridge University Press, 1987.

[12] R. Murray, Z. Li, and S. Sastry, *A mathematical introduction to Robotic Manipulation*. 1994.

[13] T. Patterson and H. Lipkin, "Structure of robot compliance," *Journal of Mechanical Design*, vol. 115, no. 3, pp. 576–580, 1993.

[14] M. R. Cutkosky and I. Kao, "Computing and controlling compliance of a robotic hand," *IEEE Transactions on Robotics and Automation*, vol. 5, no. 2, pp. 151–165, 1989.

[15] I. Kao and C. Ngo, "Properties of the grasp stiffness matrix and conservative control strategies," vol. 18, no. 2, pp. 159–167, 1999.

[16] S. Chen and I. Kao, "Conservative congruence transformation for joint and cartesian stiffness matrices of robotic hands and fingers," *The international Journal of Robotics Research*, vol. 19, pp. 835–847, sep 2000.

[17] M. Malvezzi, G. Gioioso, G. Salvietti, D. Prattichizzo, and A. Bicchi, "Syngrasp: a matlab toolbox for grasp analysis of human and robotic hands," in *Proc. 2013 IEEE International Conference on Robotics and Automation*, (Karlsruhe, Germany), pp. 1088–1093, 2013.